Membrane Location of Spin-Labeled Apocytochrome *c* and Cytochrome *c* Determined by Paramagnetic Relaxation Agents

Margot M. E. Snel,[‡] Ben de Kruijff,[§] and Derek Marsh*[,‡]

Abteilung Spektroskopie, Max-Planck-Institut für biophysikalische Chemie, Postfach 2841, D-37018 Göttingen, Germany, and Department of Biochemistry of Membranes, Centre for Biomembranes and Lipid Enzymology, Utrecht University, Padualaan 8, 3584 CH Utrecht, The Netherlands

Received April 11, 1994; Revised Manuscript Received July 7, 1994[⊗]

ABSTRACT: The mitochondrial precursor protein horse heart apocytochrome *c* was spin-labeled on the cysteine residue at position 14 or 17 in the N-terminal region, and the mature protein yeast cytochrome *c* was similarly labeled on the single free cysteine residue at position 102 at the C-terminal. The proteins were bound to negatively charged phospholipid bilayers, and the accessibility of the spin-labeled cysteine residues to lipid-soluble molecular oxygen and to the lipid-impermeant chromium oxalate anion was determined from the saturation properties of the ESR spectra. Binding of the protein was found to have a considerable effect on the local oxygen concentrations within the lipid bilayer. The accessibilities of the spin-labeled proteins relative to those obtained for phospholipids spin-labeled either in the headgroup or at positions in the *sn*-2 acyl chain, in the presence of unlabeled protein, identify the position of the spin-labeled cysteine residues in the phospholipid bilayer. The spin label on apocytochrome *c* bound to phosphatidylglycerol bilayers lies between the 5- and 14-C positions of the lipid acyl chain. Admixture of ≥75 mol % phosphatidylcholine induces an additional surface-associated apocytochrome *c* population. The spin label on native and heat-denatured cytochrome *c* is located at the membrane surface. These different extents of membrane penetration correlate also with the reduction in local oxygen concentration experienced by spin-labeled phospholipids on binding of apo- and holocytochrome *c*. The possible biological implications of the data are discussed.

Apocytochrome *c* is the heme-free precursor of mitochondrial cytochrome *c* and is synthesized in the cytoplasm. To reach its final functional location in the mitochondrion, the apoprotein has to cross the outer mitochondrial membrane. Subsequently, the heme group is attached to the cysteine residues of the N-terminal region by the enzyme heme lyase in the intermembrane space, upon which the protein then folds into the native cytochrome *c*. Data on mitochondrial import suggest that apocytochrome *c* uses a unique pathway, not taken by any other mitochondrial precursor characterized so far [for a review, see Stuart and Neupert (1990)]. No protein receptors on the mitochondrial surface are involved in the import of apocytochrome *c*. Neither does the precursor possess a cleavable presequence, nor does it need a transmembrane potential to translocate across the membrane. Biochemical and biophysical studies on the interactions of apocytochrome *c* with model membranes have revealed that the basic precursor protein binds strongly to negatively charged phospholipids (Rietveld et al., 1983), upon which a considerable perturbation of the lipid packing and lipid mobility takes place (Görrissen et al., 1986; Jordi et al., 1990; Muga et al., 1991a). Furthermore, it has been shown that apocytochrome *c*, but not cytochrome *c*, can translocate at least partially across anionic phospholipid bilayers (Dumont & Richards, 1984; Rietveld et al., 1986; Jordi et al., 1989a). Taken together, these studies provide strong indications that lipid–protein interactions can play an important role in the import of apocytochrome *c* into mitochondria.

Recently, attempts have been made to elucidate at least part of the molecular import mechanism. Studies on apocytochrome *c* associated with detergents that mimic phospholipids revealed a highly dynamic, partially folded structure for apocytochrome *c* located at the water–lipid interface (de Jongh et al., 1992; Vincent & Gallay, 1991; Snel et al., 1991). Studies of the effects of apocytochrome *c*–phospholipid interactions on the protein structure have indicated that the apoprotein possibly exists in two membrane-associated forms: one in which it is located at the surface of the membrane and one in which it penetrates partially into the lipid bilayer (Muga et al., 1991a; Berkhout et al., 1987). In the present study, the location of the N-terminal portion of apocytochrome *c* on its association with negatively charged phospholipid bilayer membranes is investigated directly by determining the accessibility of membrane-bound spin-labeled apocytochrome *c* to paramagnetic relaxation agents that are soluble either in the aqueous phase or in the hydrophobic membrane interior. For this purpose, apocytochrome *c* was spin-labeled specifically at one of the cysteine residues (position 14 or 17) in the N-terminus, which is the part of the apoprotein that has to penetrate the outer mitochondrial membrane in order for it to interact with the heme lyase. This modification of apocytochrome *c* by spin-labeling has been found not to affect the conformational characteristics and bilayer-translocation capability of the apoprotein (Snel et al., 1994).

In parallel, native yeast cytochrome *c*, which is thought not to penetrate the membrane as deeply as does apocytochrome *c* (Görrissen et al., 1986; Jordi et al., 1989a), was also investigated. For these studies, yeast cytochrome *c* was spin-labeled at the single free cysteine residue at position 102 in its C-terminal part, a modification that has been shown not to change the properties of native yeast cytochrome *c* (Drott et al., 1970; Zuniga & Nall, 1983). Several studies with model membranes have suggested that the heat-denatured form of cytochrome *c* behaves similarly to apocytochrome *c* with

* To whom correspondence should be addressed.
‡ Max-Planck-Institut.
§ Utrecht University.
⊗ Abstract published in *Advance ACS Abstracts,* August 15, 1994.

0006-2960/94/0433-11150$04.50/0

respect to its interaction with lipids (Demel et al., 1989; Jordi et al., 1990). To obtain information on the location of the C-terminus of membrane-bound apocytochrome *c*, spin-labeled yeast cytochrome *c* therefore was denatured by heat treatment and used as a model for apocytochrome *c*.

The position of the spin label on the protein in the membrane-bound form was determined from the exposure of the nitroxide spin label to paramagnetic relaxation agents by using continuous wave (CW)[1] power saturation ESR spectroscopy. The relaxation agents, molecular oxygen and chromium oxalate, were used earlier to determine the membrane topography of bacteriorhodopsin and of melittin (Altenbach & Hubbell, 1988; Altenbach et al., 1989a,b, 1990), and they also have been calibrated by using spin-labeled phospholipids (Snel & Marsh, 1993). Oxygen dissolves preferentially in the hydrophobic interior of the membrane (Subczynski & Hyde, 1981, 1983, 1984), whereas the anionic chromium oxalate is restricted to the aqueous phase (Berg & Nesbitt, 1979; Yager et al., 1979). Changes in the nitroxide relaxation times on interaction with the faster relaxing paramagnetic species are a measure of their accessibility to the nitroxide group. In this way, the location of the spin-labeled proteins was determined in membranes of negatively charged dioleoyl- and dimyristoylphosphatidylglycerols and mixtures with zwitterionic phosphatidylcholine.

EXPERIMENTAL PROCEDURES

Materials. DMPG was synthesized from DMPC (Fluka, Buchs, Switzerland) according to the method of Comfurius and Zwaal (1977). DOPG was obtained from Avanti (Birmingham, AL). Cytochrome *c* from horse heart (type VI) and from *Saccharomyces cerevisiae* (bakers' yeast) were obtained from Sigma (St. Louis, MO). Phosphatidylglycerols spin-labeled either at the 5- or at the 14-position in the *sn*-2 chain (5- and 14-PGSL, respectively) were synthesized by B. Angerstein, as described in Marsh and Watts (1982). Phosphatidic acid spin-labeled at the phosphate of the lipid headgroup (T-PASL) was prepared by H. Eibl and A. Watts at this Institute, according to the method of Eibl (1978). Potassium tris(oxalato)chromate(III) trihydrate (CROX) was synthesized as described by Bailar and Jones (1939) and characterized by its absorption spectrum (Malati & Abdul Azim, 1959, 1960). Apocytochrome *c* was prepared by removal of the heme group from horse heart cytochrome *c* (Fisher et al., 1973). Subsequently, the (labeled) apoprotein was subjected to the renaturation procedure described by Hennig and Neupert (1983), and aliquots of the renatured proteins (0.5 or 1.0 mg at a concentration of ~1.7 mg/mL) in 10 mM HEPES, 50 mM NaCl, pH 7.0, and 0.01%, v/v, 2-mercaptoethanol were stored in liquid nitrogen and used only once, immediately after thawing on ice. Heat-denatured horse heart and yeast cytochrome *c* and heat-denatured spin-labeled yeast cytochrome *c* were produced by incubating the solutions of the native proteins at a concentration of 1.9 mg/mL for 1 h at 95 °C. After cooling, the solutions were centrifuged (15000*g*, 3 min) to remove any aggregated protein.

Spin-labeled apocytochrome *c* and yeast cytochrome *c* were prepared by reacting the cysteine residues of the proteins with 3-maleimido-2,2,5,5-tetramethyl-pyrrolidine N-oxyl (5-MSL, Aldrich, Milwaukee, WI) as described previously (Snel et al., 1994). Any disulfide-bridged dimers were dissociated by prior treatment with dithiothreitol. Spin-labeled apocytochrome *c* finally was subjected to the renaturation procedure described above. The labeling levels were ~0.2 mol of 5-MSL/mole of apocytochrome *c* with the spin label attached to the cysteine residue at either position 14 or 17 and ~0.15 mol of 5-MSL/mole of yeast cytochrome *c* with the spin label attached to the cysteine residue at position 102.

In experiments with the headgroup spin label (T-PASL) and unlabeled apocytochrome *c*, indications were obtained of a possible partial reduction of the T-PASL by the cysteine residues in the apoprotein. Therefore, in these experiments apocytochrome *c* was alkylated with *N*-ethylmaleimide (NEM) according to the method given above.

ESR Sample Preparation. All experiments, except those with yeast cytochrome *c*, were performed in a buffer containing 10 mM HEPES and 50 mM NaCl, pH 7.0. For the samples containing spin-labeled or unlabeled yeast cytochrome *c*, a buffer consisting of 10 mM HEPES and 150 mM NaCl, pH 7.0, was used in order to obtain lipid/protein ratios comparable to those with the other proteins. (The reason for this latter reproducible result is not entirely understood.) For experiments in the presence or in the absence of oxygen, buffers were saturated either with oxygen or with argon, and sample tubes and ESR capillaries were flushed with oxygen or argon, respectively. Excess supernatant and sample were removed from the pellets in the ESR capillaries to obtain samples ≤5 mm in length, so as to avoid inhomogeneities of the microwave and modulation fields in the ESR cavity [cf. Fajer and Marsh (1982)]. The capillaries were sealed after flushing with either oxygen or argon.

For preparation of lipid dispersions, a dry lipid film was prepared from 1 mg of DMPG or 0.5 mg of DOPG and 1 mol % spin-labeled lipid, with 0.1 mol % butylated hydroxytoluene to prevent lipid peroxidation. This was then hydrated with respectively 50 or 25 μL of buffer and put through 5 cycles of freezing and thawing. After incubation at 37 °C for 30 min, the samples were transferred to 1-mm i.d. ESR capillaries and concentrated by centrifugation (1000*g*, 10 min).

For preparation of lipid–protein samples, a protein solution that contained a mass of protein equal to that of the lipid was added to the lipid dispersion. The samples were incubated for 30–40 min at 37 °C, and the resulting protein–lipid complexes were collected by centrifugation. Where required, the argonated lipid–protein complexes were resuspended further in 1 mM CROX freshly dissolved in argonated buffer. Subsequently, the samples were transferred to 1-mm i.d. ESR capillaries and concentrated further by centrifugation.

For samples containing only spin-labeled protein, 0.16 mM spin-labeled apocytochrome *c* or 0.45 mM spin-labeled yeast cytochrome *c* solutions were flushed with oxygen or argon and transferred to 1-mm i.d. ESR capillaries (sample length ≤ 5 mm). Protein solutions containing 1 mM CROX were prepared by diluting the argonated solutions of spin-labeled proteins with 5 mM CROX buffer (at a ratio of 4:1, v/v).

After the ESR measurements, the lipid–protein complexes were dissolved in 25 μL of 1 M NaOH. The phospholipid concentration was determined by the method of Eibl and Lands (1969), and the protein content was assayed according to the modified method of Lowry (Peterson, 1977), with bovine serum albumin as standard.

[1] Abbreviations: CW, continuous wave; ESR, electron spin resonance; DOPG, 1,2-dioleoyl-*sn*-glycero-3-phosphoglycerol; DMPG, 1,2-dimyristoyl-*sn*-glycero-3-phosphoglycerol; DMPC, 1,2-dimyristoyl-*sn*-glycero-3-phosphocholine; *n*-PGSL, 1-acyl-2-[*n*-(4,4-dimethyloxazolidine-*N*-yl)-stearoyl]-*sn*-glycero-3-phosphoglycerol; T-PASL, 4-phosphatidyl-2,2,6,6-tetramethylpiperidine-1-oxyl; NEM, *N*-ethylmaleimide; 5-MSL, 3-maleimido-2,2,5,5-tetramethylpyrrolidine-*N*-oxyl; CROX, potassium tris(oxalato)chromate(III) trihydrate; HEPES, 4-(2-hydroxyethyl)-1-piperazineethanesulfonic acid; FTIR, Fourier transform infrared spectroscopy.

ESR Spectroscopy. ESR measurements were performed on a Varian E-12 Century Line 9-GHz ESR spectrometer. Sample capillaries were centered in a standard 4-mm quartz tube containing light silicone oil for thermal stability; the temperature was regulated with a pure nitrogen gas flow system. Conventional ESR spectra were recorded at various microwave powers decreasing from 180 to 0.03 mW. This corresponds to an rms microwave magnetic field, $\langle H_1^2 \rangle^{1/2}$, at the sample ranging from approximately 600 to 6 mG. A standardized sample configuration was used in all CW saturation experiments (Fajer & Marsh, 1982; Hemminga et al., 1984), and all measurements were performed under critical coupling conditions. The microwave magnetic field was calibrated by measuring the CW saturation properties of deoxygenated aqueous peroxylaminedisulfonate (Kooser et al., 1969). The microwave cavity Q was measured as described in Fajer and Marsh (1982), and corresponding corrections were made in calculating the root mean square microwave field, $\langle H_1^2 \rangle^{1/2}$, at the sample. Quantitative subtractions between spectra with two components in different proportions were performed as described by Knowles et al. (1981).

Analysis of Saturation Curves. Saturation curves were obtained for the total spectral intensity (i.e., the second integral of the first-derivative spin label ESR spectrum) as a function of the microwave magnetic field, H_1, incident at the sample. The saturation of the total integrated spectral intensity, S, is independent of inhomogeneous broadening and, for a spectrum consisting of two components A and B, is described by (Páli et al., 1993)

$$S = S_0 H_1 [f_A/(1 + \gamma^2 H_1^2 T_{1,A} T_{2,A})^{1/2} + f_B/(1 + \gamma^2 H_1^2 T_{1,B} T_{2,B})^{1/2}] \quad (1)$$

where S_0 is a normalization factor, γ is the gyromagnetic ratio of the electron, $T_{1,i}$ and $T_{2,i}$ are the spin–lattice and spin–spin relaxation times, respectively, of the spin label component i, and f_i is the fractional integrated intensity of component i in the absence of saturation, with i = A, B ($f_A + f_B = 1$). The saturation data were fit to this equation by using a nonlinear least squares method with the effective T_1T_2 products and the normalization factor as the adjustable parameters, and the fractional populations f_A and f_B obtained from spectral subtractions as input parameters. If the difference in relaxation times between the two components is not very large and/or the intensity of one of the components is small, the saturation curve cannot be distinguished from that for a single component (Páli et al., 1993). In this case, a single-component fit to the saturation curve gives a reasonable approximation for the T_1T_2 product of the dominant component.

In the presence of a fast-relaxing paramagnetic species, the spin–lattice relaxation rate, $1/T_1$, of the spin label is enhanced by an amount depending on the concentration, c, of the fast-relaxing species:

$$1/T_1 = 1/T_1^\circ + k_{RL}c \quad (2)$$

where T_1° is the value of T_1 for $c = 0$, and k_{RL} is an accessibility parameter that depends on the diffusion coefficient and cross section for collision of the fast-relaxing species in the case of the Heisenberg spin exchange interaction or on the distance of closest approach to the spin label in the case of the magnetic dipole–dipole interaction [see, e.g., Snel and Marsh (1993)]. The diffusion coefficient of the spin label is unimportant for the relaxation enhancement because it is much slower than that of the paramagnetic agents. Since for the systems of interest changes in T_2 induced by the paramagnetic species will be negligible, the T_1T_2 product obtained from the CW saturation studies is given by

$$1/T_1T_2 = 1/(T_1T_2)^\circ + (k_{RL}/T_2^\circ)c \quad (3)$$

To compare results from samples with different line widths, the accessibility must be normalized with respect to the line width, δ, which is a measure of T_2 ($\delta \sim 1/T_2^\circ$). A general accessibility parameter is defined as the difference in the reciprocal T_1T_2 product for the nitroxide group in the presence (p) and in the absence (o) of paramagnetic species, divided by the peak-to-peak line width (δ) of the $m_I = 0$ line (Snel & Marsh, 1993):

$$\text{Accessibility parameter} = [(1/T_1T_2)_p - (1/T_1T_2)_o]/\delta \qquad [\times 10^{13}\ s^{-2}\ G^{-1}] \quad (4)$$

where δ is determined under nonsaturating conditions.

RESULTS

Analysis of CW Saturation Experiments. The dependences on microwave power of the ESR spectra from spin-labeled apocytochrome *c* bound to fluid-phase DOPG bilayers, both in the presence and in the absence of oxygen, are given in Figure 1. The saturation curves for the double-integrated intensity of the spectra given in Figure 1, together with the corresponding one for the sample in 1 mM chromium oxalate, are given in Figure 2. At higher microwave powers the degree of saturation of the spin label attached to apocytochrome *c* is reduced in oxygen. This is in contrast to the situation with chromium oxalate, which has hardly any effect on the saturation of the spin-labeled protein. The quantitative relaxation enhancements were obtained by fitting the saturation curves according to eq 1, yielding effective values of $T_1T_2 = 1.5 \times 10^{-14}$ s^2 in the absence of oxygen and chromium oxalate, $T_1T_2 = 1.4 \times 10^{-14}$ s^2 in the presence of chromium oxalate, and $T_1T_2 = 5.3 \times 10^{-15}$ s^2 in the presence of oxygen. The accessibility parameters are 4.3×10^{13} s^{-2} G^{-1} for oxygen and 0.2×10^{13} s^{-2}Gauss^{-1} for chromium oxalate. A single-component fit to the saturation curve was used in this case because the proportion of the second, mobile component in the spectrum is very low.

Accessibility of Spin-Labeled Apocytochrome c in DOPG Bilayer Dispersions. To calibrate the accessibility parameters obtained for the spin-labeled protein, comparable experiments were performed with spin-labeled phospholipids. The accessibility parameters for a lipid headgroup spin label (T-PASL) and for lipids spin-labeled in the chain (5- and 14-PGSL), determined with and without unlabeled apocytochrome *c* bound to DOPG bilayers, are given in Figure 3. The accessibility of the phospholipid spin labels to oxygen is modified differentially by the bound apocytochrome *c*. The reduction in accessibility by protein binding is greatest in the region of the phospholipid headgroups and the 5-position in the acyl chain, whereas the accessibility is reduced less at the 14-position by the presence of the protein. The accessibility parameters obtained for the spin-labeled lipids in the presence of the unlabeled protein are those appropriate for interpreting data with the spin-labeled protein. Specifically, these accessibility parameters contain the correction for the altered lipid packing of the membrane and thus for changes in the membrane concentration of oxygen that is caused by the binding of the proteins. The increased bilayer packing density is indicated by the ESR spectrum of the lipid spin labels in the presence of protein (not shown). At the lipid/protein ratios used, these spectra consist essentially of single components with increased line widths and hyperfine anisotropy,

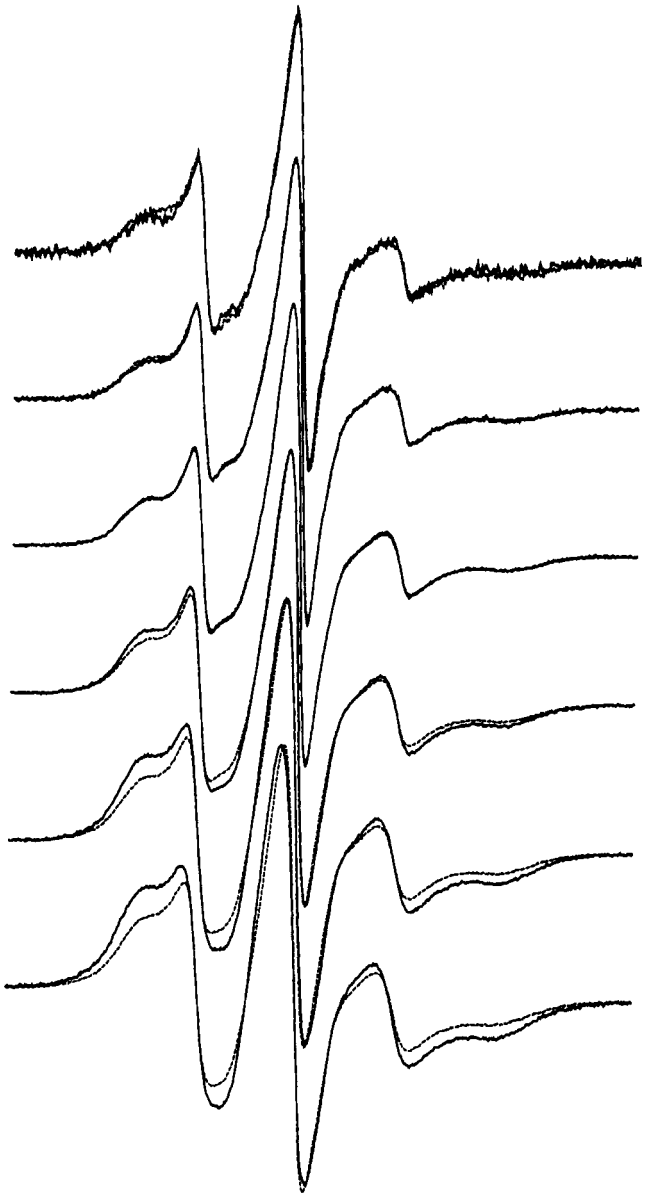

FIGURE 1: ESR spectra of spin-labeled apocytochrome *c* bound to DOPG bilayers, at a lipid/protein ratio of 14 mol/mol, in the absence (solid lines) and in the presence (dashed lines) of oxygen. From top to bottom the microwave power at which the spectra are recorded is increasing, corresponding to values of $\langle H_1^2 \rangle^{1/2} \approx 20, 59, 179, 310, 432$, and 539 mG. Spectra are normalized to the same central line height. Temperature of the sample is 30 °C. Total scan width is 100 G.

but they are still characteristic of a fluid lipid bilayer. ^{31}P NMR spectra also indicate that, at these lipid/protein ratios, the lipids are in a fluid lamellar state (Jordi et al., 1990). Similar calibrations with phospholipid spin labels in the presence of unlabeled protein were not performed for chromium oxalate because its action is limited to the aqueous phase (Altenbach et al., 1989a,b).

The accessibility parameters to oxygen and to chromium oxalate are given in Table 1 both for spin-labeled apocytochrome *c* bound to negatively charged bilayers of DOPG and for the spin-labeled protein in solution. The accessibility parameter for spin-labeled apocytochrome *c* to oxygen locates the label group on the protein at a position between the 5-PGSL and the 14-PGSL spin labels when bound to DOPG (cf. Figure 3). The low accessibility to chromium oxalate is also consistent with the spin label being buried in the membrane.

Accessibility of Spin-Labeled Apocytochrome c in DMPG/DMPC Bilayer Dispersions. The ESR spectra of spin-labeled

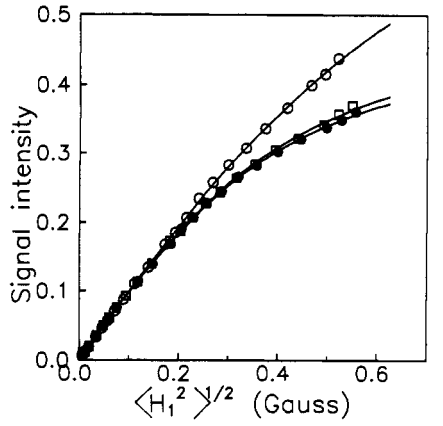

FIGURE 2: Dependence of the double-integrated intensity of the ESR spectra recorded at 30 °C, from spin-labeled apocytochrome *c* bound to DOPG bilayers in the absence (●) and in the presence (○) of oxygen and in the presence (□) of argonated 1 mM chromium oxalate, on the root mean square microwave magnetic field, $\langle H_1^2 \rangle^{1/2}$. The signal intensities are normalized relative to the number of spin labels in the samples (arbitrary units). The solid lines show the results of nonlinear least squares fits to the saturation curves according to eq 1, with rms errors of 1.7×10^{-3} (●), 1.9×10^{-3} (○), and 2.5×10^{-3} (□).

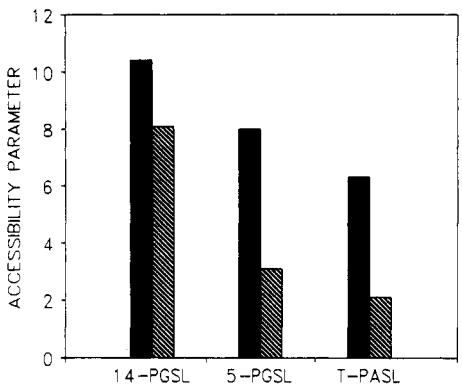

FIGURE 3: Accessibility parameters (in units of 10^{13} s^{-2} G^{-1}) for negatively charged phospholipids, spin-labeled in the headgroup (T-PASL) or at the 5- or 14-position in the *sn*-2 chain (5-PGSL and 14-PGSL, respectively), to oxygen are given for aqueous bilayer dispersions of DOPG alone (filled bars) and for DOPG dispersions with either unlabeled apocytochrome *c* or, in the case of T-PASL, NEM-labeled apocytochrome *c* bound at a lipid/protein ratio of 11 mol/mol (hatched bars). Sample temperature is 30 °C.

apocytochrome *c* bound to negatively charged bilayer membranes composed of DMPG with different mole fractions of DMPC, in the presence and in the absence of chromium oxalate, are given in Figure 4. At the low concentrations of chromium oxalate that were used in order to minimize perturbation effects, there is little paramagnetic broadening (i.e., enhanced T_2 relaxation) evident in the spectra, even at low microwave powers (data not shown). A significant feature of the spectra in Figure 4 is the increase in the proportion of the sharp, three-line, mobile spectral component with increasing DMPC content in the lipid mixtures. The fraction of the integrated intensity that this component contributes to the spectrum was obtained by intersubtractions of the spectra at low power. These results are given in Table 1. At low contents of DMPC, the contribution of the mobile component to the integrated spectral intensity is relatively small. The saturation curves then can be analyzed adequately with a single-component model to yield the accessibility parameters for the immobile component. At the higher DMPC contents, the saturation curves were analyzed using a two-component model (see Experimental Procedures). The resulting accessibilities to chromium oxalate and oxygen for spin-labeled apocyto-

Table 1: Accessibility Parameters to Oxygen and to Chromium Oxalate (CROX) for the Spin-Labeled Proteins Apocytochrome *c* (apo *c*), Yeast Cytochrome *c* (cyt *c*), and Heat-Denatured Cytochrome *c* (den. cyt *c*), in Solution and Bound to Negatively Charged Bilayers [DOPG, DMPG, and Mixtures of DMPG with DMPC at the Mole Ratios Indicated] at the Lipid to Protein Ratios (L/P) Given[a]

sample[b]	L/P (mol/mol)	*f*	accessibility parameter (10^{13} s^{-2} Gauss^{-1}) oxygen	CROX
apo *c*, 0.14 mM in buffer			2.5	5.0
DOPG–apo *c*	14	0.1	4.3	0.2
DMPG–apo *c*	13.5	0.1	1.0	1.3
DMPG/DMPC (75:25)–apo *c*	14	0.2	1.2	0.3
DMPG/DMPC (50:50)–apo *c*	22.5	0.3	2.1	0.9
DMPG/DMPC (25:75)–apo *c*[c]	38	0.55	1.9, 4.3 4.4	28.8, 4.0 7.7
DMPG/DMPC (15:85)–apo *c*[c]	58	0.6	0.5, 30.3 5.0	41.3, 7.3 14.1
cyt *c*, 0.4 mM in buffer			4.8	3.3
DOPG–cyt *c*	13		1.7	0.4
DOPG–cyt *c*	21		1.9	0.2
DOPG–den. cyt *c*	14.5		1.4	1.9

[a] Standard deviations in typical determinations of the accessibility parameter are in the region of 10–20%. *f* is the fraction of mobile spin-label component in the two-component spectra. [b] The chromium oxalate concentration in the samples is 1 mM, and they are argonated. For the experiments in the presence of molecular oxygen the samples are saturated with pure oxygen. Sample temperature is 30 °C. [c] The single values correspond to an apparent single-component fit to the saturation curves. The double values correspond to a two-component fit according to eq 1, with the values of *f* given.

chrome *c* in the DMPG–DMPC complexes are given in Table 1.

The calibration of the accessibility to oxygen for phospholipid spin labels in negatively charged bilayers of DMPG alone, in DMPG–apocytochrome *c* complexes, and in DMPG/DMPC–apocytochrome *c* complexes is given in Figure 5. Comparison of the accessibility parameters in the DMPG lipid system alone (filled bars) with those obtained when apocytochrome *c* is present (hatched bars) shows a large reduction in the accessibility to oxygen of phospholipids spin-labeled at positions from the 14-position to approximately the 5-position of the chain, whereas that for spin labels in the headgroup region (T-PASL) is less affected. The results obtained for spin-labeled phospholipids in DMPG/DMPC mixtures (15:85, mol/mol) with apocytochrome *c* bound (stippled bars) show that the effects of protein binding are mostly smaller than for DMPG alone. The largest reduction in the accessibility to oxygen is for phospholipids spin-labeled in the region from the headgroups to the 5-position, whereas phospholipids spin-labeled close to the end of the chain are not significantly affected.

The calibration for the DMPG–apocytochrome *c* system (Figure 5, hatched bars) is used to interpret the accessibility parameters to oxygen of spin-labeled apocytochrome *c* bound to bilayers composed of DMPG with mole fractions of DMPC up to 0.25. The accessibility parameters to oxygen of spin-labeled apocytochrome *c* bound to DMPG/DMPC bilayers with mole fractions of DMPC of 0.75 and 0.85 are calibrated by the DMPG/DMPC–apocytochrome *c* system from Figure 5 (stippled bars). Taking the data from Table 1, the calibrations indicate that the spin label on the protein is located in the region defined by the 5- and the 14-PGSL spin label when the protein is bound to bilayers with mole fractions of DMPC of 0 and 0.25. Correspondingly, the accessibility to chromium oxalate is low for mole fractions of DMPC up to 0.25 (Table 1), confirming that the spin label on the protein is located in the membrane. For DMPC mole fractions of 0.75 and 0.85, the proportions of mobile and immobile components in the spectra are comparable. Two-component fits to the saturation curves indicate that the accessibilities both to oxygen and to chromium oxalate are very different for the two components. These differences may be somewhat exaggerated by the fitting procedure, which requires that the saturation behavior be well separated (Páli et al., 1993). Nevertheless, they are sufficient to distinguish qualitatively between the locations of the two components. The relative values of the accessibilities, both to oxygen and to chromium oxalate, indicate that the immobile component corresponds to spin labels located in the hydrocarbon chain region of the membrane. This location of the protein is therefore similar to that for low mole fractions of DMPC. In contrast, the mobile component corresponds to spin labels at the membrane surface that are exposed to the aqueous environment. This surface-associated component either is absent or is present only at low concentration at low mole fractions of DMPC.

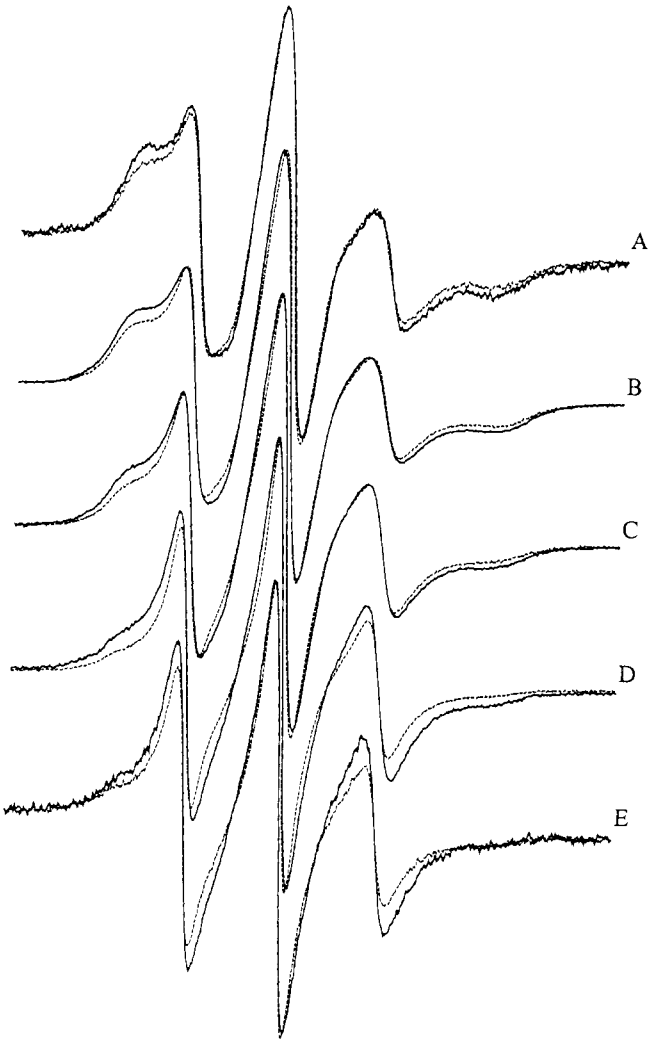

FIGURE 4: ESR spectra of spin-labeled apocytochrome *c* bound to bilayers composed of mixtures of DMPG and DMPC, at lipid/protein ratios given in Table 1, recorded at 30°C in the absence of oxygen (solid lines) and in the presence of 1 mM chromium oxalate (dashed lines) at a microwave power corresponding to $\langle H_1^2 \rangle^{1/2} \approx 500$ mG. The mole fraction of DMPC in the mixed bilayers is (A) 0, (B) 0.25, (C) 0.5, (D) 0.75, and (E) 0.85. Total scan width is 100 G.

Accessibility of Native and Denatured Spin-Labeled Yeast Cytochrome c in DOPG Bilayer Dispersions. The dependences on microwave power of the ESR spectra from spin-labeled

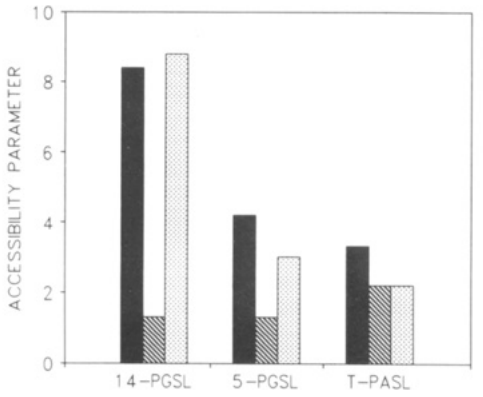

FIGURE 5: Accessibility parameters (in units of 10^{13} s^{-2} G^{-1}) for negatively charged phospholipids, spin-labeled in the headgroup (T-PASL) or at the 5- or 14-position in the *sn*-2 chain (5- and 14-PGSL, respectively), to oxygen are given for aqueous bilayer dispersions of DMPG alone (filled bars), for DMPG dispersions with unlabeled apocytochrome *c* bound at a lipid/protein ratio of 11 mol/mol (hatched bars), and for DMPG/DMPC dispersions (15:85 mol/mol) with unlabeled apocytochrome *c* bound at a lipid/protein ratio of 66 mol/mol (stippled bars). Sample temperature is 30 °C.

yeast cytochrome *c* bound to fluid-phase DOPG bilayers, both in the presence and in the absence of oxygen, are given in Figure 6. Very significant in the ESR spectra is the large immobilization of the spin label on yeast cytochrome *c* upon binding to DOPG bilayers compared to the mobile, sharp, three-line spectrum obtained for the spin-labeled holoprotein in solution (spectrum not shown).

Calibrations for the accessibility to oxygen of spin-labeled phospholipids in bilayer membranes consisting of the negatively charged DOPG alone, of DOPG with horse heart or yeast cytochrome *c* bound, and of DOPG with heat-denatured horse heart or yeast cytochrome *c* bound are given in Figure 7. In general, the horse heart and yeast cytochromes *c* have a similar effect on the accessibility parameter of the spin-labeled phospholipids to oxygen, as might be expected for closely related proteins. Comparison of the accessibility parameters obtained in the presence of cytochromes *c* with those in the lipid system alone shows that the largest reduction in oxygen accessibility is in the phospholipid headgroup region, and that this reduction gradually decreases toward the center of the membrane. The oxygen accessibility parameter of 14-PGSL in the presence of cytochrome *c* is comparable to that for 14-PGSL in DOPG alone. The reduction in the accessibility parameters to oxygen in the presence of the heat-denatured cytochromes *c* is larger, in general, than for the corresponding native proteins. At around the 14-position of the lipid chains, the accessibility to oxygen is reduced by the heat-denatured proteins, to an even greater extent than is observed for the apoprotein (cf. Figure 3).

The accessibility parameters to oxygen and to chromium oxalate of spin-labeled yeast cytochrome *c* that is bound to DOPG bilayers at lipid/protein ratios of 13 and 21 mol/mol; of heat-denatured spin-labeled yeast cytochrome *c* bound to DOPG at a lipid/protein ratio of 14.5 mol/mol; and of the spin-labeled holoprotein in solution are given in Table 1. The relatively high accessibility parameter to oxygen, and the relatively low one to chromium oxalate, that is observed for spin-labeled yeast cytochrome *c* in solution compared with those for spin-labeled apocytochrome *c* in solution is noteworthy. This indicates that the location of the spin label that is attached to the cysteine residue at position 102 in the C-terminus of yeast cytochrome *c* is not exposed to the aqueous phase to as great an extent as is found for the spin label on apocytochrome *c*, which is in a random coil form in solution. Probably the spin label on yeast cytochrome *c* is in a

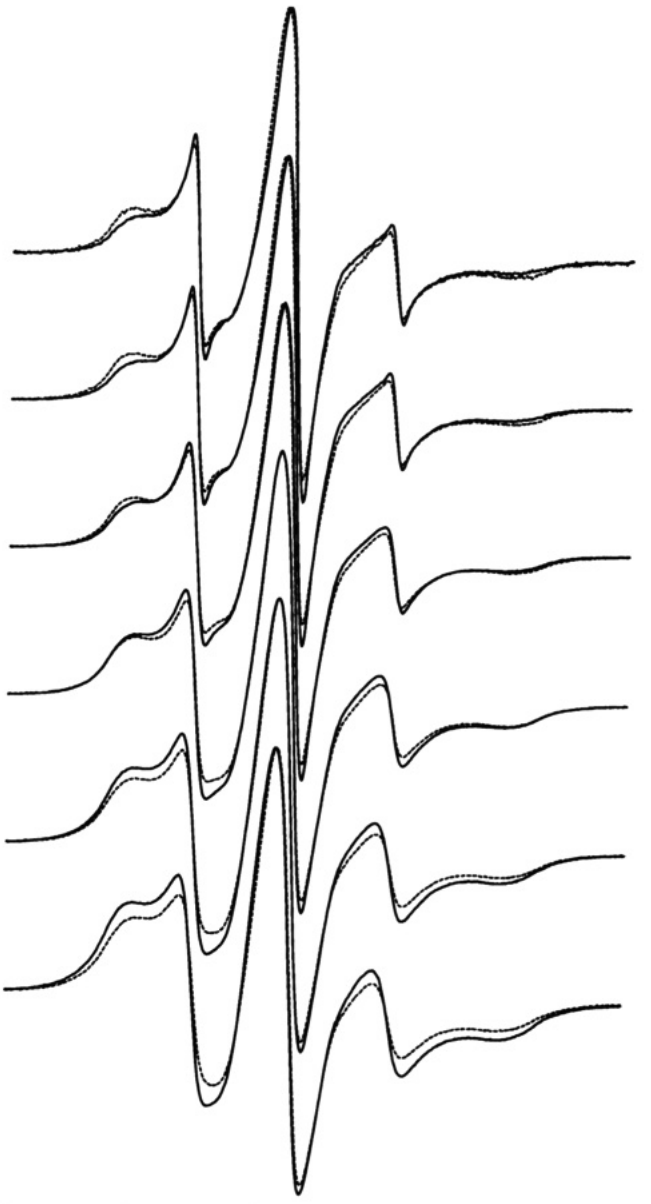

FIGURE 6: ESR spectra of spin-labeled yeast cytochrome *c* bound to DOPG bilayers, at a lipid/protein ratio of 13 mol/mol, in the absence (solid lines) and in the presence (dashed lines) of oxygen. From top to bottom the microwave power at which the spectra are recorded is increasing, corresponding to values of $\langle H_1^2 \rangle^{1/2} \approx 24$, 72, 216, 375, 523, and 652 mG. Spectra are normalized to the same central line height. Temperature of the sample is 30°C. Total scan width is 100 G.

hydrophobic pocket, such that it experiences a higher oxygen concentration and a lower accessibility to chromium oxalate. The relatively low accessibility parameters to oxygen of membrane-bound spin-labeled yeast cytochrome *c* indicate that the spin-label group is located in the phospholipid headgroup region (cf. Figure 7), which agrees with the low accessibility parameters to chromium oxalate, assuming that this region is shielded from the paramagnetic ion by binding of the protein. When spin-labeled yeast cytochrome *c* is denatured by heat treatment and is bound to the membrane, the accessibility parameters observed are indicative also of a location of the spin-label group in the phospholipid headgroup region.

Finally, it is possible to use the data in Table 1 to assess the possible effects of the surface electrostatics on the accessibility to anionic chromium oxalate. With one exception, the samples listed have comparable ratios of negatively charged lipid to protein that also are comparable to the net positive

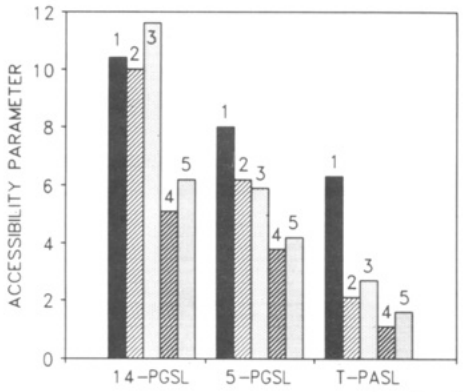

FIGURE 7: Accessibility parameter (in units of 10^{13} s^{-2} G^{-1}) for negatively charged phospholipids, spin-labeled in the headgroup (T-PASL) or at the 5- or 14-position in the *sn*-2 chain (5- and 14-PGSL, respectively), to oxygen are given for aqueous bilayer dispersions of DOPG alone (filled bars, 1), for DOPG dispersions with horse heart cytochrome *c* bound at a lipid/protein ratio of 13 mol/mol (lightly hatched bars, 2), for DOPG dispersions with yeast cytochrome *c* bound at a lipid/protein ratio of 16 mol/mol (lightly stippled bars, 3), for DOPG dispersions with heat-denatured horse heart cytochrome *c* at a lipid/protein ratio of 14 mol/mol (heavily hatched bars, 4), and for DOPG dispersions with heat-denatured yeast cytochrome *c* at a lipid/protein ratio of 14 mol/mol (heavily dotted bars, 5). Sample temperature is 30 °C.

charge on the protein. Therefore, there is a considerable degree of neutralization of the surface membrane electrostatics. In general, the accessibilities to chromium oxalate do not correlate with the residual surface charge, e.g., for 100% and 75% DMPG with apocytochrome *c*, or for native and denatured cytochrome *c* with DOPG. Also, the cytochrome *c*/DOPG samples are at a higher ionic strength, but at L/P = 13–14.5 they still have low chromium oxalate accessibilities. Hence, it appears that the values for chromium oxalate reflect rather more true accessibilities than simple electrostatic effects. It will be noted, however, that for apocytochrome *c* in buffer an electrostatic enhancement is expected. Therefore the true calibration value should be lower when compared with the membrane samples at 25% and 15% DMPG for which electrostatic neutralization is almost complete.

DISCUSSION

The location of the spin label on apo- and holocytochrome *c* and denatured cytochrome *c* in association with negatively charged phospholipid membranes has been investigated directly by determining the accessibility of the spin-label site to molecular oxygen and to anionic chromium oxalate. The calibration experiments performed on the accessibility of spin-labeled lipids to oxygen emphasize the importance of taking into account lipid–protein interactions in determining the local concentrations of this paramagnetic relaxation agent. These effects also give further information on the degree of penetration of the protein into the membrane. Particularly in the case of apocytochrome *c*, these studies are relevant with regard to its mechanism of import into mitochondria. The spin label is bound to the N-terminus of the apoprotein at the position where the heme group is attached by the heme lyase which resides in the mitochondrial intermembrane space. Therefore analysis of the membrane location of the spin label on apocytochrome *c* in the different lipid systems gives insight into the putative role of the membrane lipids in the import mechanism of apocytochrome *c* into mitochondria. However, first the location of spin-labeled yeast cytochrome *c* is analyzed, which provides a frame of reference for the application of the method to the studies on apocytochrome *c*.

Location of Native and Denatured Yeast Cytochrome c Bound to Lipid Bilayers. Spin-labeled yeast cytochrome *c* is found to be situated in the phospholipid headgroup region of DOPG bilayers, which is compatible with observations of a mainly electrostatic binding of the protein without penetration into the membrane (Rietveld et al., 1983; Görrissen et al., 1986). Significantly, it is also found that binding of holocytochrome *c* has little effect on the local oxygen concentration at the 14-C atom of the lipid chain, whereas it has a pronounced effect in the phospholipid headgroup region. It is likely that the spin label attached at position 102 in the C-terminal helix (residues 88–103) of yeast cytochrome *c* undergoes a change of location on binding the protein to the membrane—from being directed toward the protein interior to being directed toward the membrane surface—because this is accompanied by a large decrease in the mobility evident from the spin label spectral line shapes (Figure 6). Recently, Muga et al. (1991b) and Heimburg and Marsh (1993) have reported a lipid-mediated loosening and/or destabilization of the tertiary structure of cytochrome *c* upon binding of the protein to DOPG, which would be consistent with a possible rearrangement of the C-terminal helix.

The spin-label group attached at the C-terminal of heat-denatured yeast cytochrome *c* is found to be positioned in the phospholipid headgroup region of DOPG bilayer membranes, although it is somewhat more accessible to chromium oxalate than is the label on the native protein. C-Terminal fragments of apocytochrome *c* have been demonstrated to penetrate negatively charged phospholipid bilayers, although they did not reduce the mobility of so large a lipid population as did the N-terminal fragments (Jordi et al., 1989b). The present experiments would suggest that the C-terminal end of the C-terminal α-helix of apocytochrome *c* at the position of residue 102 does not penetrate the bilayer to a great extent, if heat-denatured cytochrome *c* can be taken as a good model for the apoprotein. This is in agreement with the location of tyrosine-97 at the surface of SDS micelles as determined by photo-CIDNP ^{1}H NMR (Snel et al., 1991). These data do not exclude, however, that the N-terminal section of the C-terminal helix of apocytochrome *c* inserts in phospholipid bilayers. It is significant that the binding of heat-denatured cytochrome *c* reduces the local oxygen concentration at the 14-position of the lipid chain to an extent at least as great as does that of apocytochrome *c*. This lends support to the idea that the heat-denatured protein penetrates the bilayer to a similar extent as does the apoprotein.

Location of Apocytochrome c Bound to Lipid Bilayers. The spin label on the N-terminus of the apoprotein is located between the positions of the 14-PGSL and 5-PGSL spin labels when it is bound to DOPG bilayer membranes. When the apoprotein is bound to mixed DMPG/DMPC bilayers containing 0 and 25 mol % DMPC, the spin-label group on apocytochrome *c* also is found to be positioned in the region corresponding to that between the 14-PGSL and 5-PGSL spin labels. In all these cases, the accessibility to chromium oxalate of the spin-labeled apocytochrome *c* is low, supporting the results obtained by the accessibility to oxygen.

In the mixed DMPG/DMPC bilayers with a high proportion of the zwitterionic component, 75 and 85 mol % DMPC, the apocytochrome *c* has two binding modes. This is evidenced by the strongly two-component nature of the ESR spectra from the spin-labeled protein. One binding mode is similar to that in DOPG and in DMPG/DMPC mixtures with low DMPC content. The other binding mode corresponds to apocytochrome *c* associated at the surface of the bilayer. The very high apparent accessibilities to chromium oxalate in this latter mode most probably correspond to specific binding to the membrane-associated protein. In support of this, the

relaxation enhancement of spin-labeled apocytochrome *c* bound to DMPG/DMPC (15:85, mol/mol) was found to be saturable. The accessibility parameter increased only slightly on going from 1 to 10 mM chromium oxalate and then remained constant up to 50 mM. This saturable interaction almost certainly is attributable to the high positive charge density on the surface-bound apocytochrome *c*. The neutral Ni-iminodiacetic acid paramagnetic complex did not give rise to such high relaxation enhancements in these samples [cf. also Snel and Marsh (1993)].

Two different binding modes for apocytochrome *c* associated with membranes containing a high proportion of zwitterionic lipid were proposed earlier by Muga et al. (1991a) and by Berkhout et al. (1987). The direct evidence provided by the ESR experiments for the coexistence of two differently located populations of membrane-bound apocytochrome *c* is in accord with studies on intact mitochondria. Simultaneous accessibility of bound apocytochrome *c* has been found both to externally added proteases and to the heme lyase which is located in the space between the outer and inner mitochondrial membrane (Nicholson et al., 1988).

Conclusions. The N-terminus of apocytochrome *c* is located partially in the lipid bilayer and partially at the surface of the membrane when the membrane contains a proportion of negatively charged lipid (15–25 mol %) that resembles that of the negatively charged lipid components in the outer mitochondrial membrane [cf. Hovius et al. (1990)]. Apocytochrome *c* is found to be positioned deep in the lipid bilayers when these contain only phosphatidylglycerols, hence illustrating the membrane-insertion propensity of the N-terminus of apocytochrome *c*, as was reported previously (Jordi et al., 1989a,b, 1990). Additionally, a considerable perturbation of the lipid packing and of the lipid mobility occurs upon binding of apocytochrome *c* to negatively charged lipid bilayers (Görrissen et al., 1986; Muga et al., 1991a). Taken together, the spontaneous partial insertion of the apoprotein might facilitate the interaction with the heme lyase, which is located in the mitochondrial intermembrane space and attaches the heme group to the apoprotein, upon which the apoprotein folds into holocytochrome *c*. Therefore, the spontaneous insertion of the N-terminus of apocytochrome *c* into the lipid bilayer, as is observed directly in this study, might trigger the import of apocytochrome *c* into mitochondria.

ACKNOWLEDGMENT

We thank B. Angerstein for expert technical help, Drs. H. Eibl and A. Watts for the synthesis of one of the spin labels, and Dr. T. Páli for the programs used in analyzing the saturation curves.

REFERENCES

Altenbach, C., & Hubbell, W. L. (1988) *Proteins 3*, 230–242.
Altenbach, C., Flitsch, S. L., Khorana, H. G., & Hubbell, W. L. (1989a) *Biochemistry 28*, 7806–7812.
Altenbach, C., Froncisz, W., Hyde, J. S., & Hubbell, W. L. (1989b) *Biophys. J. 56*, 1183–1191.
Altenbach, C., Marti, T., Khorana, H. G., & Hubbell, W. L. (1990) *Science 248*, 1088–1092.
Bailar, J. C., Jr., & Jones, E. M. (1939) *Inorg. Synth. 1*, 35–38.
Berg, S. P., & Nesbitt, D. M. (1979) *Biochim. Biophys. Acta 548*, 608–615.
Berkhout, T. A., Rietveld, A., & de Kruijff, B. (1987) *Biochim. Biophys. Acta 897*, 1–4.
Comfurius, P., & Zwaal, R. F. A. (1977) *Biochim. Biophys. Acta 488*, 36–42.
De Jongh, H. H. J., Killian, J. A., & de Kruijff, B. (1992) *Biochemistry 31*, 1636–1643.
Demel, R. A., Jordi, W., Lambrechts, H., van Damme, H., Hovius, R., & de Kruijff, B. (1989) *J. Biol. Chem. 264*, 3988–3997.
Drott, H. R., Lee, C. P., & Yonetani, T. (1970) *J. Biol. Chem. 245*, 5875–5879.
Dumont, M. E., & Richards, F. M. (1984) *J. Biol. Chem. 259*, 4147–4156.
Eibl, H. (1978) *Proc. Natl. Acad. Sci. U.S.A. 75*, 4074–4077.
Eibl, H., & Lands, W. E. M. (1969) *Anal. Biochem. 30*, 51–57.
Fajer, P., & Marsh, D. (1982) *J. Magn. Reson. 49*, 212–224.
Fisher, W. R., Taniuchi, H., & Anfinsen, C. B. (1973) *J. Biol. Chem. 248*, 3188–3195.
Görrissen, H., Marsh, D., Rietveld, A., & de Kruijff, B. (1986) *Biochemistry 25*, 2904–2910.
Heimburg, T., & Marsh, D. (1993) *Biophys. J. 65*, 2408–2417.
Hemminga, M. A., de Jager, P. A., Marsh, D., & Fajer, P. (1984) *J. Magn. Reson. 59*, 160–163.
Hennig, B., & Neupert, W. (1983) *Methods Enzymol. 97*, 261–274.
Hovius, R., Lambrechts, H., Nicolay, K., & de Kruijff, B. (1990) *Biochim. Biophys. Acta 1021*, 217–226.
Jordi, W., Li-Xin, Z., Pilon, M., Demel, R. A., & de Kruijff, B. (1989a) *J. Biol. Chem. 264*, 2292–2301.
Jordi, W., de Kruijff, B., & Marsh, D. (1989b) *Biochemistry 28*, 8998–9005.
Jordi, W., de Kroon, A. I. P. M., Killian, J. A., & de Kruijff, B. (1990) *Biochemistry 29*, 2313–2321.
Knowles, P. F., Watts, A., & Marsh, D. (1981) *Biochemistry 20*, 5888–5894.
Kooser, R. G., Volland, W. V., & Freed, J. H. (1969) *J. Chem. Phys. 50*, 5243–5257.
Malati, M. A., & Abdul Azim, A. A. (1959) *Egypt. J. Chem. 2*, 47.
Malati, M. A., & Abdul Azim, A. A. (1960) *Chem. Abstr. 54*, 2085f.
Marsh, D., & Watts, A. (1982) in *Lipid–Protein Interactions* (Jost, P. C., & Griffith, O. H., Eds.) Vol. 2, pp 53–126, Wiley-Interscience, New York.
Muga, A., Mantsch, H. H., & Surewicz, W. K. (1991a) *Biochemistry 30*, 2629–2635.
Muga, A., Mantsch, H. H., & Surewicz, W. K. (1991b) *Biochemistry 30*, 7219–7224.
Nicholson, D. W., Hergersberg, C., & Neupert, W. (1988) *J. Biol. Chem. 263*, 19034–19042.
Páli, T., Horváth, L. I., & Marsh, D. (1993) *J. Magn. Reson. A101*, 215–219.
Peterson, G. L. (1977) *Anal. Biochem. 83*, 346–356.
Rietveld, A., Sijens, P., Verkleij, A. J., & de Kruijff, B. (1983) *EMBO J. 2*, 907–913.
Rietveld, A., Jordi, W., & de Kruijff, B. (1986) *J. Biol. Chem. 261*, 3846–3856.
Snel, M. M. E., & Marsh, D. (1993) *Biochim. Biophys. Acta 1150*, 155–161.
Snel, M. M. E., Kaptein, R., & de Kruijff, B. (1991) *Biochemistry 30*, 3387–3395.
Snel, M. M. E., de Kruijff, B., & Marsh, D. (1994) *Biochemistry 33*, 7146–7156.
Stuart, R. A., & Neupert, W. (1990) *Biochimie 72*, 115–121.
Subczynski, W. K., & Hyde, J. S. (1981) *Biochim. Biophys. Acta 643*, 283–291.
Subczynski, W. K., & Hyde, J. S. (1983) *Biophys. J. 41*, 283–286.
Subczynski, W. K., & Hyde, J. S. (1984) *Biophys. J. 45*, 743–748.
Vincent, M., & Gallay, J. (1991) *Eur. J. Biophys. 20*, 183–191.
Yager, T. D., Eaton, G. R., & Eaton, S. S. (1979) *Inorg. Chem. 18*, 725–727.
Zuniga, E. H., & Nall, B. T. (1983) *Biochemistry 22*, 1430–1437.